Nanotechnology

PAPER

Hyperthermia-triggered release of hypoxic cell radiosensitizers from temperature-sensitive liposomes improves radiotherapy efficacy *in vitro*

IOP Publishing Nanotechnology

Nanotechnology **30** (2019) 264001 (13pp) https://doi.org/10.1088/1361-6528/ab0ce6

Hyperthermia-triggered release of hypoxic cell radiosensitizers from temperature-sensitive liposomes improves radiotherapy efficacy *in vitro*

Negar Sadeghi[1,2,3], Robbert Jan Kok[2], Clemens Bos[1], Maurice Zandvliet[4], Willie J C Geerts[5], Gert Storm[1,2,6], Chrit T W Moonen[1], Twan Lammers[3,6,7] and Roel Deckers[1,7]

[1] Imaging Division, University Medical Center Utrecht, Utrecht, The Netherlands
[2] Department of Pharmaceutics, Utrecht Institute for Pharmaceutical Sciences, Utrecht University, Utrecht, The Netherlands
[3] Department of Nanomedicine and Theranostics, Institute for Experimental Molecular Imaging, University Clinic and Helmholtz Institute for Biomedical Engineering, RWTH Aachen University, Aachen, Germany
[4] Department of Clinical Sciences of Companion Animals, Faculty of Veterinary Medicine, Utrecht University, The Netherlands
[5] Biomolecular Imaging, Bijvoet Center, Utrecht University, Utrecht, The Netherlands
[6] Department of Targeted Therapeutics, MIRA Institute for Biomedical Technology and Technical Medicine, University of Twente, Enschede, The Netherlands

E-mail: tlammers@ukaachen.de and R.Deckers-2@umcutrecht.nl

Received 4 December 2018, revised 15 February 2019
Accepted for publication 5 March 2019
Published 12 April 2019

Abstract

Hypoxia is a characteristic feature of solid tumors and an important cause of resistance to radiotherapy. Hypoxic cell radiosensitizers have been shown to increase radiotherapy efficacy, but dose-limiting side effects prevent their widespread use in the clinic. We propose the encapsulation of hypoxic cell radiosensitizers in temperature-sensitive liposomes (TSL) to target the radiosensitizers specifically to tumors and to avoid unwanted accumulation in healthy tissues. The main objective of the present study is to develop and characterize TSL loaded with the radiosensitizer pimonidazole (PMZ) and to evaluate the *in vitro* efficacy of free PMZ and PMZ encapsulated in TSL in combination with hyperthermia and radiotherapy. PMZ was actively loaded into TSL at different drug/lipid ratios, and the physicochemical characteristics and the stability of the resulting TSL–PMZ were evaluated. PMZ release was determined at 37 °C and 42 °C in HEPES buffer saline and fetal bovine serum. The concentration-dependent radiosensitizing effect of PMZ was investigated by exposing FaDu cells to different PMZ concentrations under hypoxic conditions followed by exposure to ionizing irradiation. The efficacy of TSL–PMZ in combination with hyperthermia and radiotherapy was determined *in vitro*, assessing cell survival and DNA damage by means of the clonogenic assay and histone H2AX phosphorylation, respectively. All TSL–PMZ formulations showed high encapsulation efficiencies and were stable for 30 d upon storage at 4 °C and 20 °C. Fast PMZ release was observed at 42 °C, regardless of the drug/lipid ratio. Increasing the PMZ concentration significantly enhanced the effect of ionizing irradiation. Pre-heated TSL–PMZ in combination with radiotherapy caused a 14.3-fold increase in cell death as compared to radiotherapy treatment alone. In conclusion, our results indicate that TSL–PMZ in

[7] Authors to whom any correspondence should be addressed.

combination with hyperthermia can assist in improving the efficacy of radiotherapy under hypoxic conditions.

Keywords: nanomedicine, hyperthermia, radiotherapy

1. Introduction

Hypoxia is a characteristic feature of solid tumors and an important cause of resistance to radiotherapy [1–4]. Ionizing radiation kills cells by causing DNA damage via direct ionization of the DNA or indirectly via free radical formation (i.e. mainly radiolysis of water) [5]. Whereas in the presence of oxygen peroxides are formed in the DNA that permanently 'fix' the DNA damage, under hypoxic conditions the DNA damage can be restored to its pre-irradiated state [6].

Several approaches such as hyperbaric oxygen [7], carbogen breathing with nicotinamide [8–10], hypoxia activated prodrugs [11] and hypoxic cell radiosensitizers have been pursued to overcome the hypoxia problem and increase the radiation effects. Among these methods, nitroimidazole compounds, the most important class of hypoxic cell radiosensitizers, have been extensively studied [12–14]. Nitroimidazoles sensitize hypoxic tumor cells by mimicking the effect of oxygen in the radiochemical process (i.e. DNA damage fixation) [15–17]. In contrast to oxygen, these radiosensitizers are not rapidly metabolized by the tumor cells and, consequently, are able to penetrate better into the tumor core to reach the hypoxic cells [18, 19]. A meta-analysis of randomized clinical studies in which nitroimidazoles were given with primary radiotherapy showed that the addition of radiosensitizers significantly improved the locoregional tumor control after radiotherapy, especially for head and neck cancer [20]. Unfortunately, dose-limiting side effects like neurotoxicity prevent their widespread use in the clinic [21–23].

The present study addresses the encapsulation of nitroimidazole radiosensitizers in tumor-targeted nanomedicines. Nanomedicines can be used to target drugs specifically to tumors and avoid unwanted distribution of radiosensitizers to healthy tissues [24, 25]. Such an approach can potentially reduce (neuro)toxic side effects and can, at the same time, substantially promote the efficacy of radiation therapy. The tumor specific accumulation of nanomedicines is due to the so-called enhanced permeability and retention (EPR) effect [26, 27]. The EPR effect is mediated by the pathophysiological vascular structure and function in solid tumors enabling the accumulation of nanoparticles in tumor tissue [28, 29]. However, the EPR effect is a highly heterogeneous phenomenon with substantially intra- and inter-tumor- and intra- and inter-patient-variability. Furthermore, inefficient release of the drug from nanomedicines present in tumors can lead to a low bioavailability of the drug in the tumor tissue.

To overcome these drawbacks, we propose to encapsulate radiosensitizers in temperature-sensitive nanoparticles, which are not dependent on EPR-phenomena for tumor accumulation. In contrast, these systems allow for rapid intravascular release of their contents upon applying regionally confined heat. Fast intravascular release of drugs from temperature sensitive liposomes (TSL) leads to elevated intravascular drug concentrations for as long as the tumor is heated and drug-loaded TSL pass the area. This high drug concentration gradient drives diffusion of the drug from the vascular space into the tumor interstitium, ultimately leading to elevated tumor drug levels [30, 31]. For example, ThermoDox® (Celsion Corporation, Columbia, MD, USA), doxorubicin encapsulated in thermosensitive liposomes, releases the drug rapidly upon mild hyperthermia [32]. This fast temperature-triggered release of doxorubicin from TSL in the tumor vasculature leads to 3–25 times higher tumor drug concentrations along with significant improvements of treatment efficacy compared to commercial doxorubicin-liposomes formulation (i.e. Doxil®/Caelyx®) and non-liposomal (i.e. aqueous) doxorubicin [33, 34]. To the best of our knowledge, this approach has only been used to trigger the release from chemotherapeutic agents until now.

In the present study, we developed and characterized TSL loaded with the radiosensitizer pimonidazole (PMZ), a nitroimidazole analog. The developed nanomedicine formulation of pimonidazole will allow us to investigate a new concept (i.e. local radiosensitizer delivery) in which the radiosensitizer is released by a stimulus confined to the tumor, to improve the efficacy of radiotherapy while reducing systemic toxicity (figure 1). We have studied the *in vitro* stability and temperature-dependent drug release properties of pimonidazole-loaded temperature sensitive liposomes (TSL–PMZ). Furthermore, we have evaluated *in vitro* the efficacy of PMZ and TSL–PMZ in combination with hyperthermia as radiosensitizing drugs for conventional radiotherapy.

2. Material and methods

2.1. Materials

Phospholipids 1,2-dipalmityol-sn-glycero-3-phosphocholine (DPPC), 1,2-distearoyl-sn-glycero-3-phosphoethanolamine-N-PEG2000 (DSPE-PEG2000) were provided by Lipoid (Ludwigshafen, Germany). 1-stearoyl-2-hydroxy-sn-glycero-3-phosphocholine(MSPC) was purchased from Avanti Polar Inc. (Alabaster, AL, USA). Other chemical reagents were purchased from Sigma Aldrich unless otherwise specified.

2.2. Preparation of liposomes loaded with PMZ

Lysolipid containing TSL were prepared by the lipid film hydration and extrusion method [35]. Liposomal encapsulation of PMZ was done by active loading. The TSL–PMZ was composed of DPPC:MSPC:DSPE-PEG2000 with a mole ratio of 86:10:4. Briefly, phospholipids (PLs, total amount 300 μmol) were dissolved in chloroform: methanol (9:1 v/v) solution. The solvent was removed using a rotary evaporator

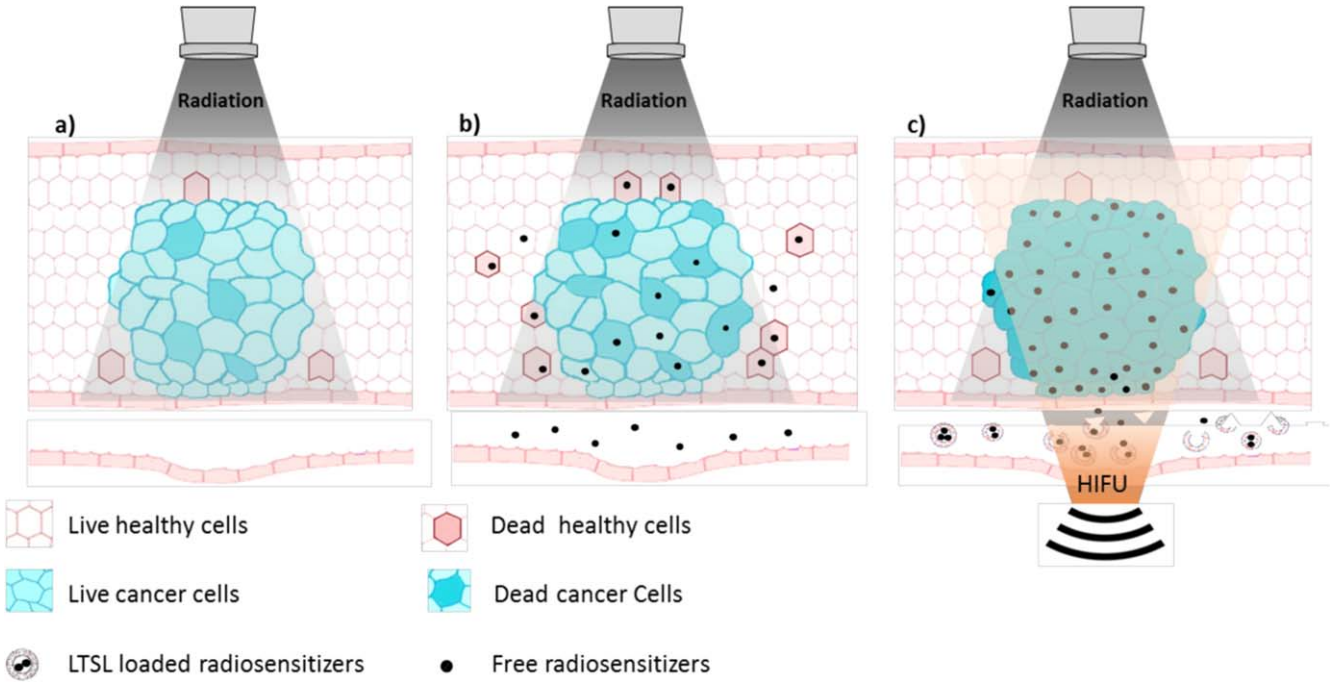

Figure 1. Schematic representation of cell killing effect of radiotherapy on tumor and healthy cells following exposure to the radiation. (a) Without using hypoxic radiosensitizers: only a limited number of tumor cells are killed due to hypoxia-induced radio-resistance. (b) Using hypoxic radiosensitizers: although the presence of hypoxic radiosensitizers increases the amount of hypoxic tumor cells that are killed, it also increases the damage of healthy tissue. (c) Using TSL-loaded hypoxic radiosensitizers: hypoxic radiosensitizers are released from temperature sensitive liposomes following local application of hyperthermia (i.e. HIFU) in and around the tumor. As a result, more tumor cells are killed by irradiation, while the toxicity for healthy cells remains unchanged.

until a thin and homogenous lipid film was formed and subsequently flushed with nitrogen to remove any other traces of organic solvents. For active loading of PMZ, the lipid film was first hydrated with 10 ml of 200 mM ammonium sulfate buffer solution (pH 5.5) at 60 °C for 30 min, resulting in a PL concentration of 30 mM, and extruded over 650, 200 and 100 nm polycarbonate filters (5 times each, 60 °C). Next, the extra-liposomal solution was replaced by dialysis with HEPES Buffered Saline pH 7.4 (HBS; 20 mM HEPES, 150 mM NaCl). Subsequently, PMZ aqueous solution was added to the liposome dispersion at different drug-to-lipid (D/L) ratios (i.e. 0.100, 0.050, 0.030 and 0.025) and incubated at 37 °C for 90 min. Finally, un-encapsulated drug was removed from TSL–PMZ by size exclusion chromatography using PD-10 desalting column (GE Healthcare, Europe GmbH) equilibrated with HBS pH 7.4. The resulting liposomes were stored at 4 °C until further use.

2.3. Liposome characterization

The mean size and polydispersity of the liposomes were determined by dynamic light scattering (ALV CGS-3, Langen, Germany) at 25 °C ± 1 °C. The zeta potential of the liposomes was determined in 10 mM HEPES buffer pH 7.4 with the laser Doppler micro-electrophoresis method using a Zetasizer Nano-Z (Malvern Instruments Ltd., Worcestershire, United Kingdom). The onset temperature (T_{onset}) and phase transition temperature (T_m) of the LTSL-PMZ 0.050 were measured with differential scanning calorimetry (DSC; Discovery, TA Instruments, USA). Liposomes were diluted in HBS or 90% fetal bovine serum (FBS) and transferred into aluminum pans (T zero hermetic aluminum pans) and sealed with lids. The appropriate reference solutions were HBS or FBS. Samples were thermally scanned from 35 °C to 45 °C at 0.5 °C min^{-1} heating rate.

The encapsulation efficiency (EE) was determined by calculating the ratio of total PMZ concentration before and after free (i.e. un-encapsulated) drug removal by PD-10 desalting column:

$$EE(\%) = (C_{after}/C_{before}) \times 100,$$

where C is the PMZ concentration of the liposome suspension after liposome lysis with acetonitrile. PMZ concentrations were determined by HPLC (see below) in triplicate. The stability of the liposomes was evaluated by measuring size and PMZ retention after 10, 20 and 30 d storage at 4 °C and 20 °C.

Cryo-transmission electron microscopy (Cryo-TEM) was used to characterize the structure of the TSL–PMZ liposomes and the physical state of the encapsulated PMZ. TSL–PMZ and empty TSL were diluted with HBS to reach a final phospholipid concentration of 1 mg ml^{-1}. Three microliters of the liposome samples were placed on the surface of a glow discharged QUANTIFOIL Micromachined Holey Carbon (R 2/2) TEM grid (Quantifoil Micro Tools, Jena, Germany) held by a Vitrobot Mark IV tweezer (Thermo Fisher Scientific). The Vitrobot environmental chamber was equilibrated at room temperature and 100% humidity. Blotting conditions were chosen such that a 100–500 nm liquid specimen film spanning holes of the grid will form. Excess sample fluid was

removed by blotting filter paper. Specimens were plunged into liquid ethane at its freezing point, where the thin specimen films were vitrified, followed by transfer under liquid nitrogen into a 626 single tilt liquid nitrogen cryo holder (Gatan, Munich, Germany). A Tecnai 20 electron microscope (Thermo Fisher Scientific) with a LaB6 filament was used at 200 keV to evaluate the specimens. Specimen temperature was maintained below −170 °C. An Eagle 4k × 4k CCD camera (Thermo Fisher Scientific) was used under normal or low-dose (nominal defocus of 2 μm) conditions to record images. Gray value averages (± standard deviation) of pixels inside and immediately outside individual vesicles ($n = 75$) were determined using the IMOD software package (version 4.8.39). Statistical significance was determined by the Student's T-test.

2.4. Determination of PMZ concentration

Reversed-phase high-performance liquid chromatography (HPLC) was used to determine PMZ concentration in samples. PMZ was separated using a C18 column (4.6 × 150 mm, 5 μm, Sunfire column) with an isocratic mobile phase containing of Acetonitrile (HPLC grade)/Water (Milli-Q) (20:80, v/v) with 0.1% (v/v) perchloric acid (HPLC grade) and detected by a spectrophotometric detector (λ: 325 nm). 10 μl per sample was injected and eluted with a flow rate of 1 ml min^{-1}, the column was maintained at 50 °C. A calibration curve (5–500 μg ml^{-1}) was prepared from PMZ stock solution diluted in HBS and used to quantify PMZ concentration based on the peak area.

2.5. Time and temperature triggered release of PMZ

The time-dependent release of PMZ from the TSL–PMZ with different D/L ratios was determined after incubation of the dispersions (in HBS) in a water bath (Memmert, GmbH, Germany) at 37 °C and 42 °C. Incubation periods were 0.5, 1, 2, 5, 10, 30 and 60 min at both temperatures. Similarly, temperature-dependent PMZ release was measured after 5 min incubation at temperatures in the range of 35 °C–45 °C. Briefly, 10 μl of the TSL suspensions were added to an Eppendorf containing 90 μl HBS or FBS pre-heated at the desired temperature and incubated in the water bath for the defined duration. Next, the sample was put on ice and 400 μl HBS of 4 °C was added.

To separate the free PMZ fraction from the liposome-encapsulated PMZ fraction, reversed-phase solid phase extraction technique was used. Briefly, a Supel^{TM}-Select HLB column (Sigma Aldrich, 54181-U, 30 mg) was conditioned with 6 × 500 μl of methanol followed by 6 × 500 μl HBS (flow rate of 0.5 ml min^{-1}). Subsequently, the column was saturated with phospholipids using 10 mg of empty TSL. The column sorbent was maintained in a wet state at all times. Following the column conditioning, 500 μl of cooled sample containing the liposomal and/or free PMZ was added to the top of the column. The first eluate contained HBS and/or FBS components passing through the column together with liposomes (from here on referred as the liposome containing fraction) was collected. Subsequently, the column was further washed with 2 × 500 μl of HBS. Finally, the column was eluted with 2 × 500 μl methanol to remove the free PMZ that was retained by the column matrix material (from here on referred to as the free PMZ fraction).

In order to quantify the drug amount in the free PMZ fraction, the methanol was evaporated by a vacuum concentrator (Christ PVC 2-25) and the resulting residue was reconstituted in HBS. Finally, this solution was analyzed by HPLC as described above. The percentage of PMZ release was calculated as:

$$\text{PMZ release } \% = (C_s - C_0)/(C_{tot} - C_0) \times 100\%,$$

where C_s is the free PMZ concentration of a sample after incubation in the water bath, C_0 is the concentration of free PMZ present in the liposome dispersion before incubation and C_{tot} is the total amount of PMZ present in the liposome dispersion, as determined after precipitation of FBS proteins and disruption of the liposomes by addition of acetonitrile (1:5 v/v). The acetonitrile was evaporated using vacuum concentrator, as described above, and subsequently the PMZ powder was reconstituted in HBS.

2.6. Cell culture

Human Hypopharengeal carcinoma cells (FaDu) were obtained from ATCC® HTB-43^{TM} (LGC Standards GmbH, Wesel, Germany) and were cultured in high glucose—Dulbecco's Modified Eagle's Medium (Sigma-Aldrich, Zwijndrecht, Netherlands), supplemented with 10% FBS (Sigma-Aldrich) and 1% Non-Essential Amino Acids (Sigma-Aldrich). Cells were incubated in standard cell culture flasks at 5% CO_2, 37 °C in a well humidified incubator. At 80% confluency, the cells were sub-cultured twice per week.

2.7. Radiosensitizing effect of PMZ on hypoxic cells

The concentration-dependent radiosensitizing effects of PMZ were investigated by exposing cells to PMZ for 3 h under hypoxic conditions followed by irradiation. Forty-eight hours prior to the irradiation, 1 × 10^6 cells were seeded into T-25 flasks in order to reach 90% confluence at the moment of irradiation. Three hours prior to radiation, culture media were replaced by Opti-MEM® (ThermoFisher Scientific, Landsmeer, Netherlands) containing different concentrations of free PMZ (0, 0.25, 0.5 or 0.75 mM) and subsequently the flasks were incubated in a hypoxic incubator (37 °C, 0.1% O_2, 5% CO_2) for 3 h. As a control, one flask containing no PMZ was incubated in a normal incubator (37 °C, 5% O_2, 5% CO_2) for 3 h. Next, flasks were sealed air-tight and irradiated with a single fraction of 0–8 Gy using a linear accelerator (Elekta Precise Linear Accelerator 11F49, Elekta, Crawley, United Kingdom). The flasks were positioned on top of 2 cm polystyrene, for proper dose build-up, and submerged in a 37 °C water bath. The radiation was applied from below. After irradiation, cell survival and DNA damage were measured by clonogenic assay and phosphorylation of histone H2AX, respectively. Briefly, for the clonogenic assay, cells were removed from the T-25 flask and seeded in triplicate at

Table 1. Physicochemical properties of TSL–PMZ formulations.

Liposome formulation	Diameter (mean ± SD[a]) (nm)	PDI (mean ± SD)	Zeta potential (mean ± SD) (mV)	Encapsulation efficiency (mean ± SD) (%)	PMZ:PL ratio (mean ± SD) (w/w)	PMZ concentration (mean ± SD) (mM)
TSL–PMZ 0.100	102 ± 3	0.15 ± 0.04	−13 ± 2	52 ± 3	0.056 ± 0.002	5.78 ± 0.17
TSL–PMZ 0.050	102 ± 0	0.12 ± 0.03	−15 ± 1	85 ± 8	0.034 ± 0.001	4.42 ± 0.07
TSL–PMZ 0.030	103 ± 1	0.13 ± 0.04	−14 ± 1	83 ± 1	0.030 ± 0.001	3.26 ± 0.13
TSL–PMZ 0.025	102 ± 1	0.14 ± 0.03	−15 ± 1	89 ± 6	0.020 ± 0.000	2.45 ± 0.04

[a] SD: standard deviation; values are mean ± SD of three batches.

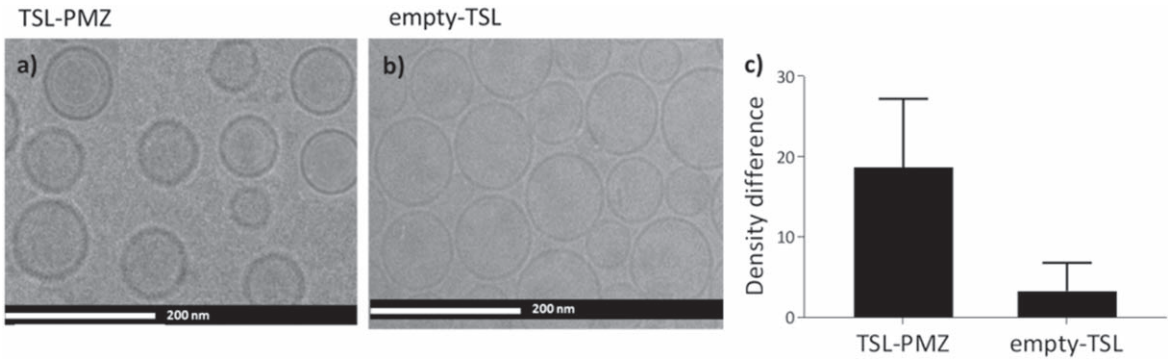

Figure 2. Cryo-transmission electron microscopy images of PMZ-loaded (a) and empty (b) TSL. The electron density difference (mean ± standard deviation) between inside and immediately outside individual vesicles ($n = 75$) was significantly ($p = 0.0001$) larger for TSL–PMZ compared to empty TSL (c).

different seeding densities, depending on the received treatment, in 6-well plates and incubated under regular culture conditions (37 °C, 5% O_2, 5% CO_2) for 2 weeks to allow the formation of colonies. Then, colonies were fixed and stained with 6% glutaraldehyde and 0.05% w/v crystal violet. Colonies of at least 50 cells were counted. The surviving fraction (SF) of all treatment groups were calculated based on the plating efficiency (PE) of the control sample (i.e. normoxic, 0 Gy, no PMZ). Subsequently, the oxygen enhancement ratio (OER) and sensitization enhancement ratio (SER) were determined using the formulas: OER $= D_0$ (hypoxic)$/D_0$ (air) and SER $= D_0$ (without sensitizer)$/D_0$ (with sensitizer), with D_0 the radiation dose that produces the same biologic effect (i.e. SF $= 0.1$).

The killing effect of radiotherapy on FaDu cells treated by different concentration of PMZ (0.25, 0.5 and 0.75 mM), was evaluated by analyzing DNA double-strand breaks (DSBs) using antibody labeling of γH2AX and flow cytometry. The untreated FaDu cells under normoxic conditions were used as a control. All groups were treated with 4 Gy radiation. For measuring the DSBs using γH2AX staining, cells were harvested 30 min after radiation and fixed in 1% PFA and permeabilized overnight in 70% ethanol at −20 °C. Subsequently, cells were blocked with 1% BSA/0.2% Triton X-100/PBS and incubated for 30 min with FITC-labeled anti-H2AX mouse IgG1 antibody (1:20; Biolegend, London, United Kingdom). After washing, a solution of 5 μg ml^{-1} propidium iodide (Sigma-Aldrich®) and 100 μg ml^{-1} RNase (ThermoFisher) was added to normalize the γH2AX signal for DNA. Finally, stained samples were measured by flow cytometry and analyzed in FlowJo software (FlowJo LLC). The percentage of γH2AX-positive cells was measured for each condition and normalized to the normoxic group.

2.8. Radiosensitizing effect of liposomal PMZ

The efficacy of liposomal PMZ in combination with radiation therapy and hyperthermia was determined by measuring cell survival and DNA damage. For this purpose, 1×10^6 cells were seeded into T-25 flasks 48 h prior to irradiation. Three hours prior irradiation, culture medium was replaced with medium that had been spiked with free PMZ (0.075 and 0.75 mM) or TSL–PMZ (0.75 mM). Spiked media had been heated at 37 °C or 42 °C for 5 min prior to addition to cells. Next, cells were incubated for 3 h under hypoxic conditions (37 °C, 0.1% O_2, 5% CO_2) and finally exposed to a single radiation dose of 4 Gy. For measuring the cell survival, the cells were harvested 30 min after radiation and seeded for clonogenic assay as described above.

3. Results and discussion

3.1. Characterization of PMZ loaded liposomes

The characteristics of all PMZ–TSL formulations are summarized in table 1. Small unilamellar liposomes were obtained with a mean size around 100 nm and low polydispersity. The D/L-ratio had no effect on the diameter of the liposomes. The zeta potential of PMZ–TSLs was in the range from −13 to −15 mV, which was also reported by others for liposome formulations consisting of DPPC, MSPC and DSPE-PEG2000 [36–38].

The active loading method using a pH gradient leads to high encapsulation efficiencies (i.e. >50%), but the EE was influenced by the D/L-ratio. This result is in agreement with other studies reporting on the remote loading method [39], The EE of PMZ with D/L-ratios of 0.050, 0.030 and 0.025 was above 80%. However, the EE of PMZ was reduced to about 52% when the D/L-ratio was 0.100. High D/L-ratios may lead to an excess of drug that exceeds the liposomal loading capacity and causes damage to the liposomal membrane, resulting drug release and thus, lower EE [40].

Cryo-TEM was used to characterize the structure of the TSL–PMZ and empty TSL and the loading of PMZ (figures 2(a), (b)). All liposome formulations primarily appeared as unilamellar spherical vesicles consisting of a lipid bilayer (higher density bands) surrounding an aqueous core. To determine the morphology of PMZ inside the liposome, the electron density inside the vesicle was compared with the surrounding medium (figure 2(c)). The electron density difference was significantly ($p = 0.0001$) larger for TSL–PMZ compared to empty TSL, 18.7 ± 8.7 versus 3.3 ± 3.5, respectively. This higher election density is consistent with

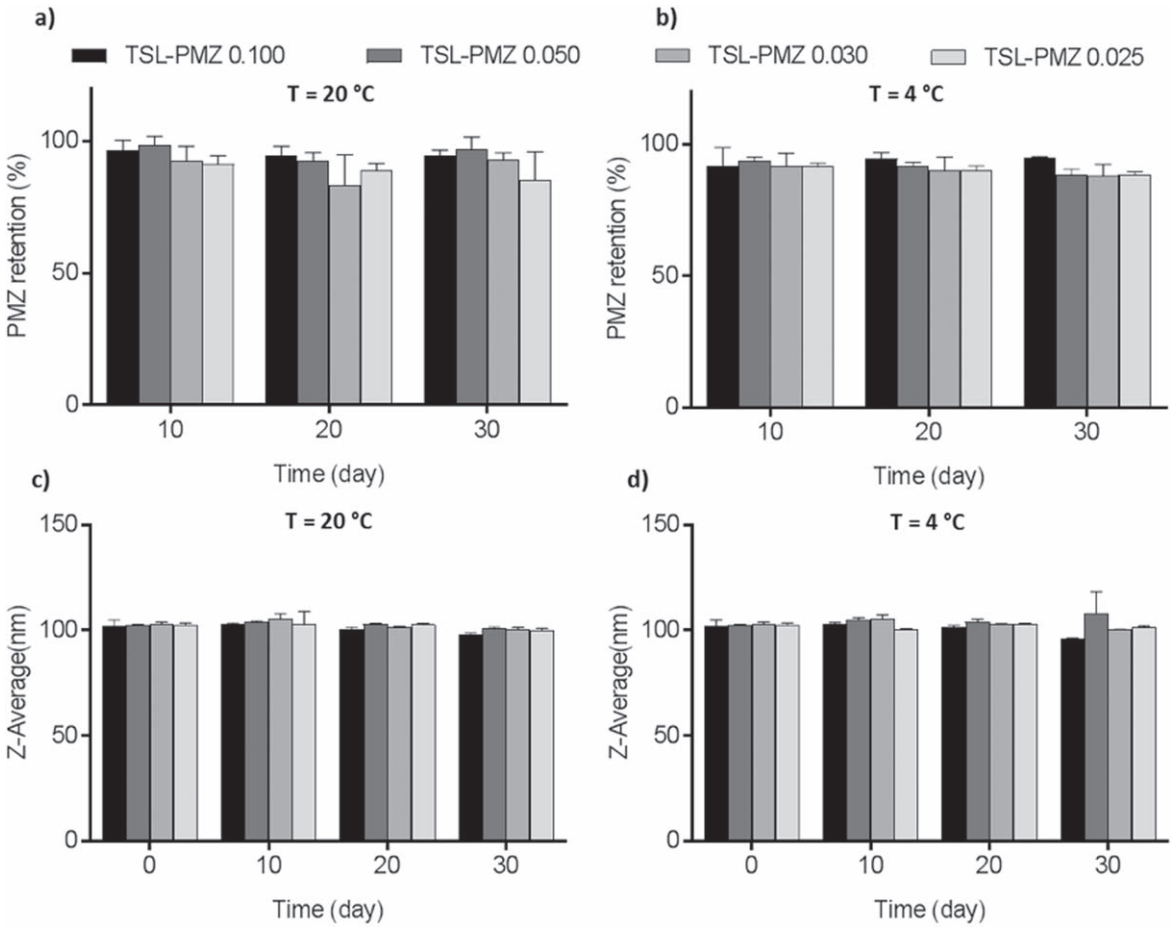

Figure 3. Stability of PMZ-loaded liposomes with different D/L ratios. The drug retention inside the liposomes (a), (b) and liposome size (Z-average) (c), (d) were measured following 10, 20 and 30 d incubation at 20 °C (a), (c) and 4 °C (b), (d) using HPLC and DLS, respectively (mean ± SD, $n = 3$).

the presence of salts like PMZ sulfate in the liposome interior. The current Cryo-TEM data do not unequivocally elucidate the physical state of the compound (i.e. dissolved or nanocrystals) since PMZ sulfate may have precipitated only after processing of the TEM samples. The morphology of liposomal PMZ is different from liposomal drugs such as doxorubicin and topotecan, where drug crystals could be seen in the liposome interior [41, 42]. It is known that the nature of the precipitate and the extent of precipitation can be affected by factors such as the type of counterion and the intravesicular pH [43].

3.2. Stability of LTSL-PMZ

The stability of all TSL–PMZ formulations during storage was evaluated by measuring the drug retention and liposome size after incubation at 4 °C and 20 °C for different durations (figure 3). All liposome formulations were stable during 30 d. Their drug retention was independent from the D/L-ratio and remained above 80% during 30 d storage at 4 °C and 20 °C (figures 3(a), (b)). Furthermore, the size of TSL–PMZ did not change over time (figures 3(c), (d)), which indicates that the liposome formulations remained physically stable. The presence of sulfate counter ions and -possibly- intraliposomal precipitation of PMZ sulfate inhibits drug efflux in actively loaded liposomes [40–44].

3.3. Time and temperature-triggered release of PMZ

The release of PMZ from TSL–PMZ with different D/L-ratios was measured as a function of incubation time at 37 °C and 42 °C in HBS (figures 4(a) and (b)). After 30 s incubation at 42 °C, about 80% of the PMZ was released from the TSL independent of the D/L-ratio. Extending the incubation time at 42 °C up to 60 min did not significantly change the amount of PMZ released. This fast PMZ release observed at 42 °C is comparable with doxorubicin release from TSL which have been reported in other studies [45, 46]. Incubation of the different TSL formulations at 37 °C up to 60 min resulted in less than 5% release, demonstrating that TSL–PMZ formulations retained very well their content at physiological temperature. Accordingly, the release-and-stability profile of TSL–PMZ is compatible with the proposed application of intravascular release by hyperthermia. The PMZ loaded TSL showed less leakage in comparison with liposomes loaded with doxorubicin [45, 47]. Since the actively loaded formulations with 0.025, 0.030 and 0.050 D/L-ratio showed similar stability and triggered release results, further

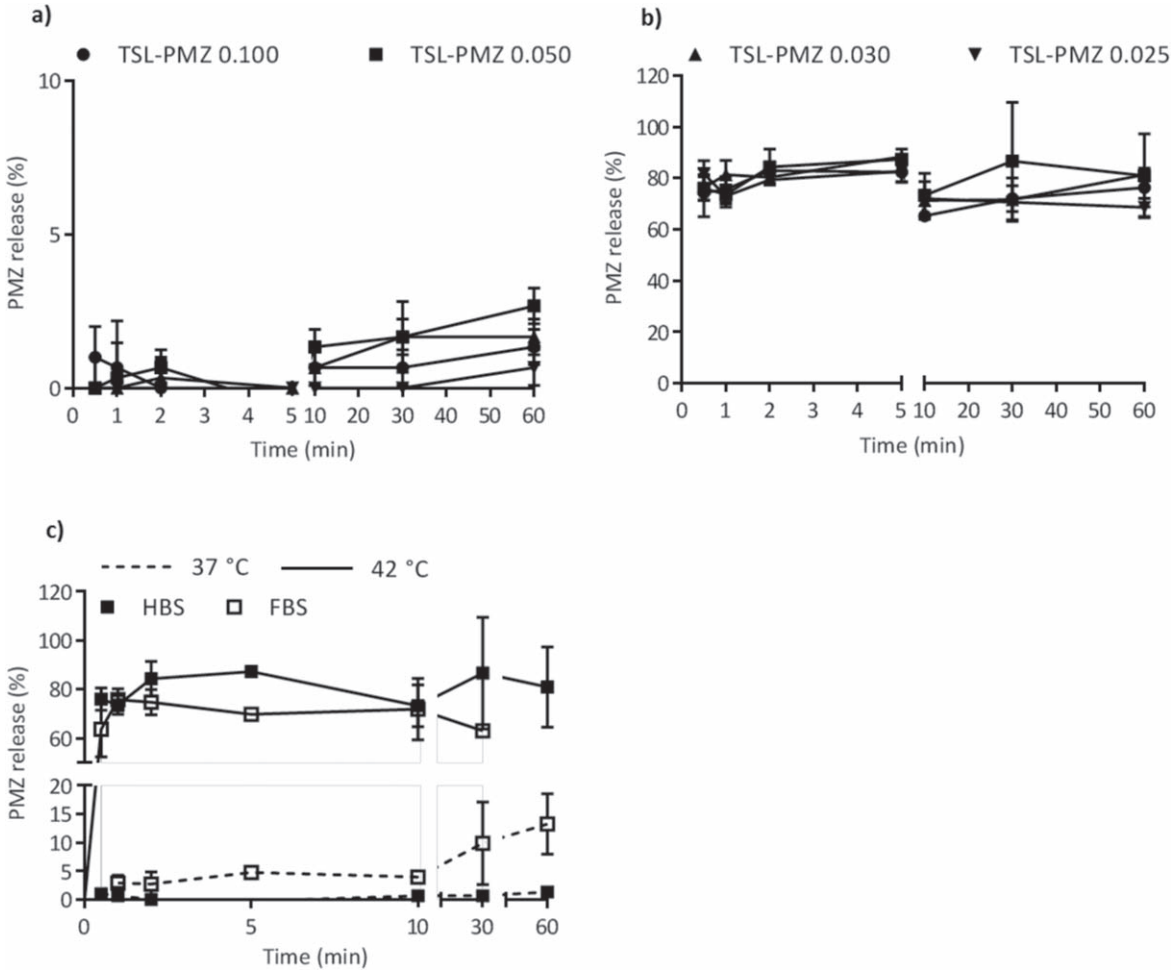

Figure 4. Temperature-triggered release of PMZ from PMZ–TSL with different D/L ratios. The release of PMZ from the different TSL–PMZ formulations was measured over 60 min upon incubation (a) at $T = 37$ °C and (b) at $T = 42$ °C in HBS. For the TSL-PMS 0.050 formulation the PMZ release was also measured over 60 min upon incubation in HBS and FBS at 37 °C and 42 °C (c). (mean ± SD, $n = 3$).

experiments were only performed with 0.050 D/L-ratio formulation.

To investigate the influence of serum compounds on the release rate, the TSL–PMZ 0.050 was also incubated at 37 and 42 °C in the presence of FBS (figure 4(c)). The PMZ release remained fast, i.e. about 80% after 30 s at 42 °C, however the leakage of PMZ at 37 °C increased to 13% after 30 min of incubation. The decreased stability of the TSL formulation in the presence of serum was also observed by other groups and might be due to the extraction of the lysolipid by plasma proteins [48].

Furthermore, the temperature-dependent PMZ release properties of TSL–PMZ 0.050 were measured for the temperature range 35 °C–45 °C in HBS and FBS (figure 5(a)). In HBS, the TSL–PMZ remained stable at temperatures up to 39 °C during 5 min, whereas in FBS, already significant PMZ release was observed at 39 °C. At 42 °C, maximum release was obtained in HBS as well as FBS. These observations correspond with the DSC data (figure 5(b)) showing a lower onset temperature (40.1 °C versus 40.9 °C) and T_m (41.1 °C versus 41.8 °C) for TSL in FBS. Similar observations were made for TSL containing doxorubicin [49, 50] and mitomycin C [51].

3.4. PMZ enhances the response of hypoxic cells to radiation exposure

To demonstrate the potential of PMZ as radiosensitizer, FaDu cells were incubated with PMZ under hypoxic conditions, and subsequently irradiated. Figure 6(a) shows the SF of cells irradiated under normoxic and hypoxic conditions. In the absence of PMZ, irradiation under hypoxic conditions reduced the radiosensitivity of FaDu cells. The oxygen enhancement ration (OER) at a 0.1 SF was 2.1, which corresponds with values typically found in literature [52, 53]. The radiation response of hypoxic cells was enhanced by irradiating the cells in the presence of PMZ (figures 6(b) and (c)). Increasing the PMZ concentration, i.e. 0.25, 0.50 and 0.75 mM, significantly enhanced the effect of ionizing radiation in a concentration-dependent way, leading to sensitization enhancement ratios (SERs) of 1.7, 2.3 and 2.9, respectively. This steep dose-response relationship was also found for misonidazole [54] and makes these compounds

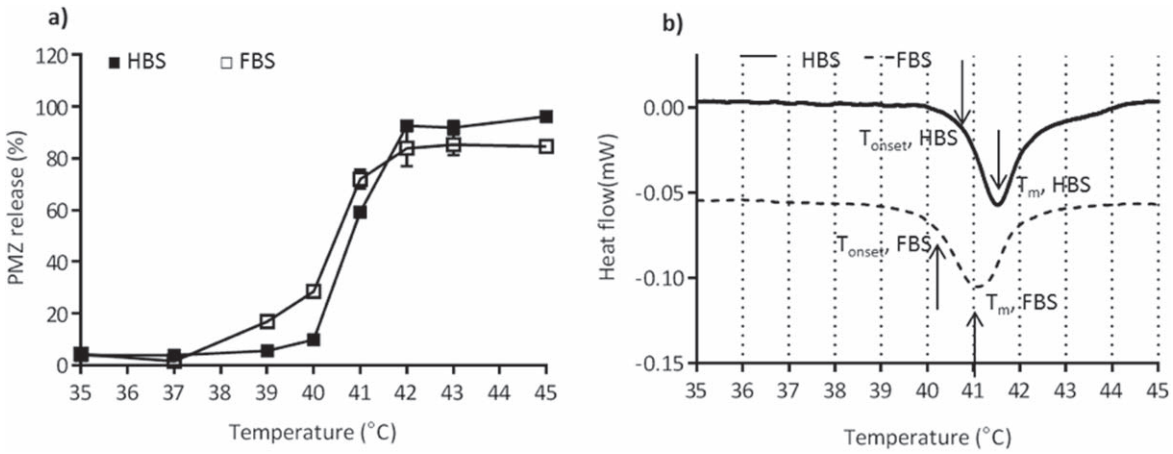

Figure 5. Temperature sensitivity of TSL–PMZ 0.050 in HBS and FBS. (a) Release profile of encapsulated PMZ from TSL incubated in HBS and FBS during 5 min at temperatures between 35 °C and 45 °C. (b) DSC thermographs of PMZ–TSL in HBS and FBS. Onset temperature (T_{onset}) and phase transition temperature (T_m) of the TSL–PMZ liposomes are indicated in panel by arrows (mean ± SD, $n = 3$).

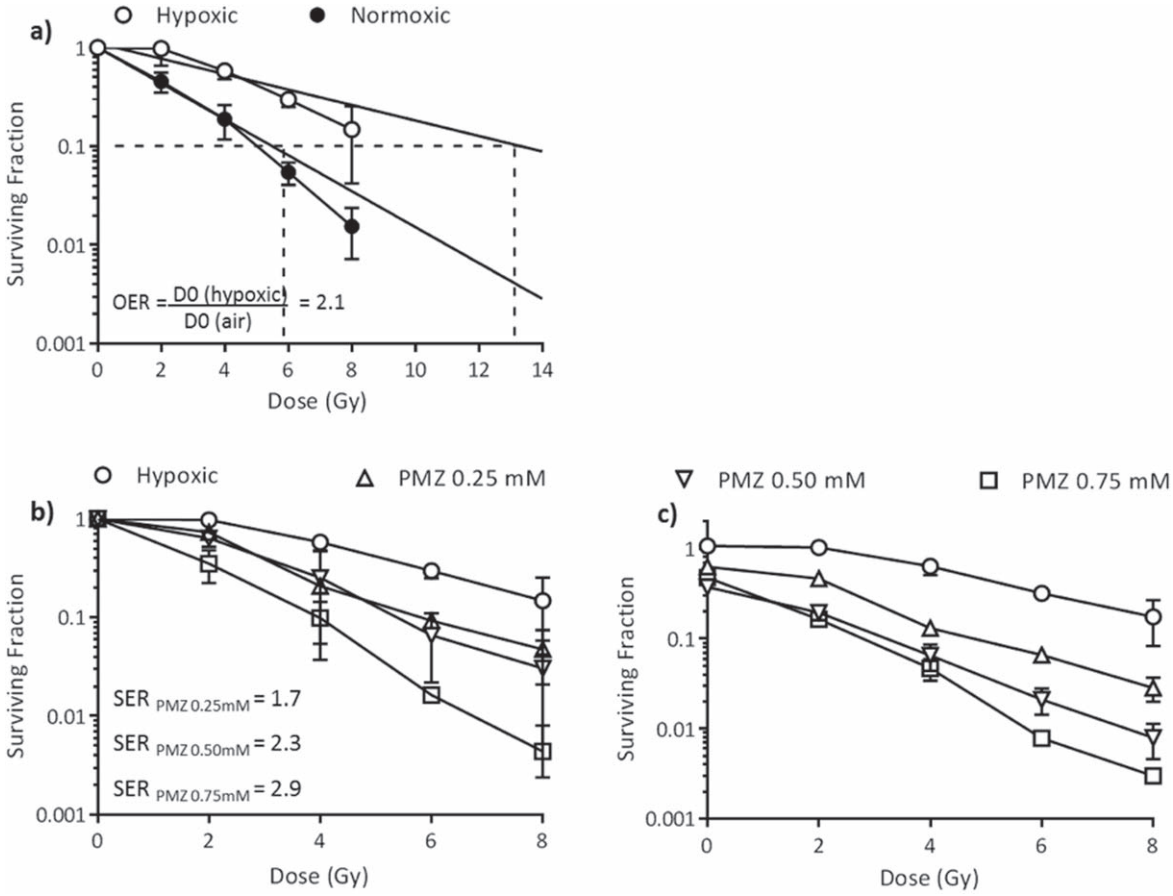

Figure 6. Survival of FaDu cells after exposure to different concentrations of PMZ for 3 h under normoxic and hypoxic conditions. The effect of (a) normoxic (5% O_2) and hypoxic (0.1% O_2) conditions on the radiosensitivity of FaDu cells expressed by the oxygen enhancement ratio (OER). (b) The effect of PMZ concentration on the radiosensitivity of FaDu cells under hypoxic conditions expressed by the sensitization enhancement ratio (SER). (c) The toxic effects of PMZ (under hypoxic conditions) in absence of radiation are visible in the non-normalized survival curves (mean ± SD, $n = 3$).

very suitable for the local radiosensitizer delivery concept. In addition, PMZ is a potent radiosensitizer given that a similar enhancement ratio of ∼1.5 is already reached at a concentration 0.25 mM compared to 1 and 10 mM for nimorazole [55] and doranidazole [56, 57], respectively. Interestingly, the radiosensitizing effect of 0.75 mM PMZ with a SER of 2.9 is larger than the radiosensitizing effect of oxygen under normoxic conditions (i.e. pO2 of 141 mmHg) with an OER of 2.1

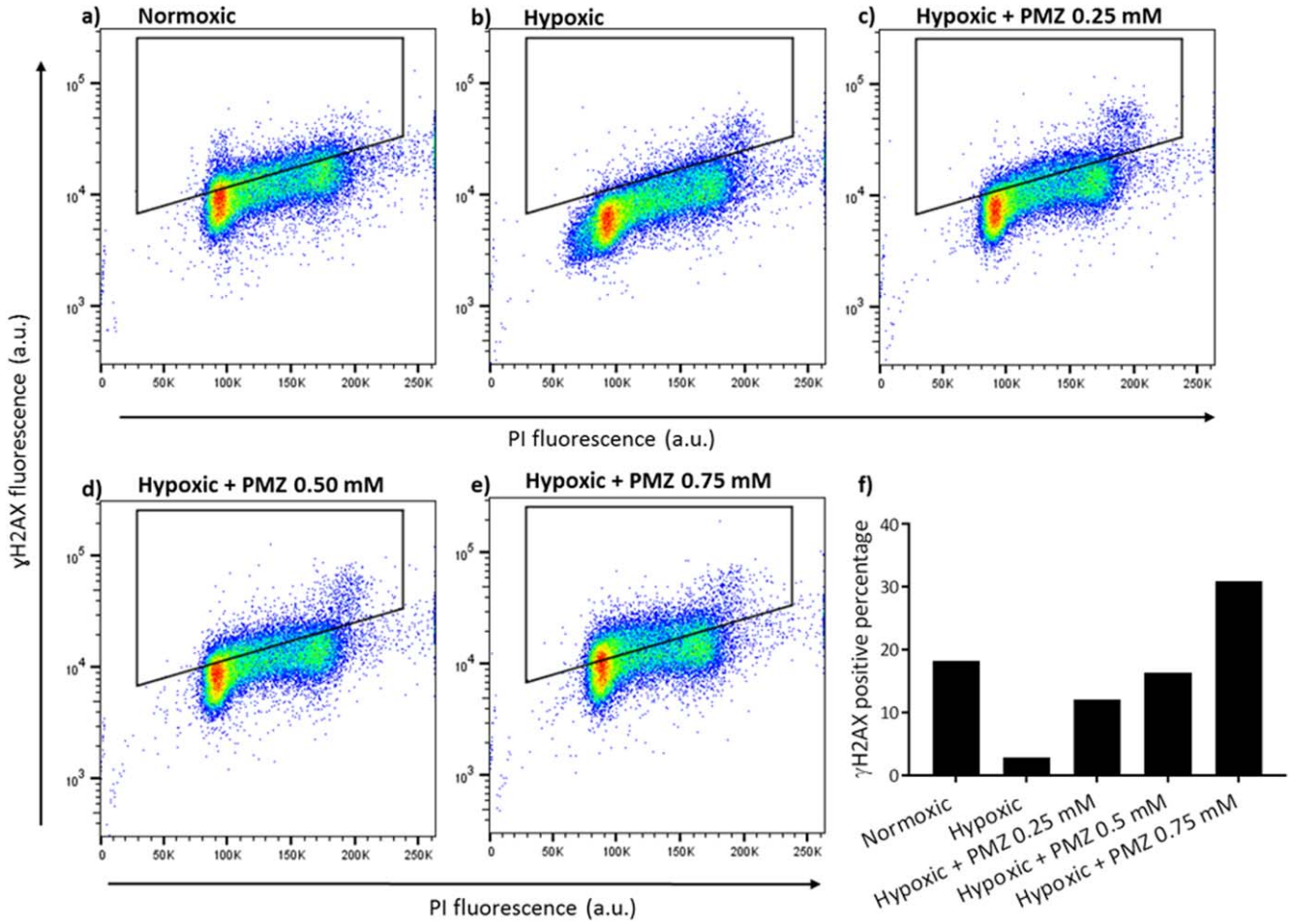

Figure 7. γH2AX positive fraction measured by flow cytometry following different treatment schedules in FaDu cells. All groups were treated with 4 Gy radiation. The percentage of γH2AX positive cells following (a) normoxic, (b) hypoxic, (c) hypoxic + PMZ 0.25 mM, (d) hypoxic + PMZ 0.5 mM and (e) hypoxic + PMZ 0.75 mM treatment from a single experiment. (f) Bar plot of the percentage γH2AX positive cells (i.e. % cells inside gate) following different treatment schedules.

and approaches the OER value of pure oxygen [58]. The non-normalized survival curves in figure 6(c) show that PMZ also has a toxic effect in the absence of radiation, leading to 52% ± 5% cell kill at 0.75 mM. Therefore, encapsulation of PMZ in the TSL will reduce the toxicity in unheated healthy tissue.

Typical concentrations achieved in human tumors after administration of misonidazole and nimorazole are in the range of 15–40 $\mu g\, g^{-1}$ tumor and lead to sensitizing effects [59]. In addition, preclinical studies in rabbits with doxorubicin-loaded TSL (i.e. ThermoDox) have shown that the i.v. infusion of ThermoDox (containing 1.8 mg doxorubicin/ml) at a dose of 5 $mg\, kg^{-1}$ in combination with local hyperthermia resulted in tumor concentrations of about 30 μg doxorubicin/g tumor [60]. Therefore, we expect that PMZ-loaded TSL (containing 1.1 mg PMZ/ml) in combination with local hyperthermia will lead to sufficient tumor concentrations that can cause radiosensitizing effects in hypoxic tumors. At the same time, the surrounding non-heated tissue will experience much lower PMZ concentrations and thus less irradiation induced damage. To confirm the results from the clonogenic assay, the DNA damage resulting from different treatments was investigated by measuring the number of double-strand breaks (DSBs) using antibody labeling of γH2AX, a marker for DSBs, by flow cytometry (figure 7). As expected, the number of DSBs (i.e. γH2AX-positive cells) is lower under hypoxic conditions compared to normoxic conditions. With increasing PMZ concentration, the number of DSBs increased. Also, in this case the number of DSBs in hypoxic cells incubated with 0.75 mM PMZ (30.9%) is larger than in normoxic cells (18.2%).

3.5. In vitro proof-of-concept of temperature-triggered radiosensitizer delivery

The effect of irradiation in combination with TSL–PMZ pre-exposed at 37 °C or 42 °C on cell death is demonstrated in figure 8. TSL–PMZ exposed to heat caused a 14.3-fold increase in radiation-induced cell death compared to radiotherapy alone. This increase in cell kill is, as expected, comparable to 3 h exposure to an equivalent concentration of free PMZ (i.e. 0.75 mM), since 5 min at 42 °C causes nearly complete release of the liposome-loaded PMZ (see figure 4(c)). In addition, others have shown that PMZ-uptake by cells reached a plateau within 30–240 min of incubation

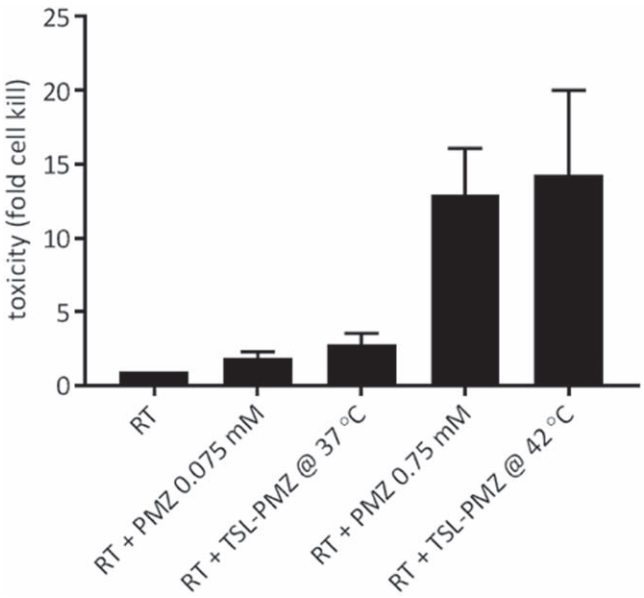

Figure 8. The toxicity of combined treatment of FaDu cells with TSL–PMZ and radiation. Cell survival was evaluated by clonogenic assay method. The cells were treated with pre-heated TSL–PMZ at 37 °C (RT + TSL–PMZ at 37 °C) and 42 °C (RT + TSL–PMZ at 42 °C) under hypoxic conditions for 3 h and radiated at 4 Gy. (mean ± SD, $n = 3$).

[61]. In contrast, TSL–PMZ which were not exposed to heat, but were incubated at 37 °C, caused only a 2.8-fold increase in cell death compared to radiotherapy without PMZ. This slight increase in cell killing effect at 37 °C can be explained by the expected leakage at this temperature, which is about 10%, and corresponds to the cell death induced by 0.075 mM free PMZ (i.e. 10% of 0.75 mM, which is the liposomal PMZ concentration). These results show that as long as the radiosensitizer is encapsulated in the TSL the radiation effects are not enhanced. Healthy tissues which are not heated are therefore expected to be protected against the direct cytotoxic effects of the radiosensitizer. Therefore, no toxicity-related problems are foreseen upon the expected accumulation of the liposomes in the liver. In addition, the liver is typically outside the irradiation beam when treating tumors in the head and neck region. Liposomes will not easily extravasate into most other tissues due to the presence of normal blood vessels with continuous endothelium and accordingly healthy tissue surrounding the tumor will not be exposed to the radiosensitizing effect of PMZ. Only in the heated tumor area, large amounts of PMZ will be present due to the triggered release process leading to a considerable increase of radiation exposure effects.

4. Conclusions

Our study shows that a radiosensitizer, i.e. PMZ, can be loaded in TSLs with high EE. Upon heating (42 °C), the TSL–PMZ will rapidly release the radiosensitizer in high amounts (i.e. 80% within 30 s). The radiosensitizing effect of PMZ was clearly dose dependent leading to double strand DNA breaks and radiation induced cell killing with increasing concentrations of PMZ. Finally, it was shown that PMZ-loaded TSLs in combination with hyperthermia improved the efficacy of radiotherapy *in vitro* under hypoxic conditions. In future studies, we aim to investigate if temperature-induced radiosensitizer delivery using TSLs will lead to high radiosensitizer concentrations in tumors and increased treatment efficacy when combined with radiotherapy. The dose dependent radiosensitizing effect of PMZ may increase the local efficacy of the radiosensitizer in combination with radiotherapy and may further reduce systemic toxicity of PMZ. Eventually, the concept of local temperature-triggered radiosensitizer delivery may provide a better radiotherapy treatment modality for hypoxic tumors.

Acknowledgments

The authors would like to thank Masha Hoogenboom, Ingrid Boots and Kim van de Berkmortel from the department Clinical Sciences of Companion Animals, division of Diagnostic Imaging for their help with irradiation experiments, Kim van der Wurff-Jacobs for her help with for the flow cytometry experiments, Joep van den Dikkenberg for his help with cell culturing, Louis van Bloois and Mies van Steenbergen for their help with preparing and characterizing liposomes and Helen Besse for help analyzing the clonogenic data. This work was supported by an ERC Advanced Grant (Sound Pharma; 268906)

ORCID iDs

Robbert Jan Kok https://orcid.org/0000-0003-4933-3968
Twan Lammers https://orcid.org/0000-0002-1090-6805

References

[1] Gray L H *et al* 1953 The concentration of oxygen dissolved in tissues at the time of irradiation as a factor in radiotherapy *Br. J. Radiol.* **26** 638–48
[2] Overgaard J 2011 Hypoxic modification of radiotherapy in squamous cell carcinoma of the head and neck–a systematic review and meta-analysis *Radiother. Oncol.* **100** 22–32
[3] Vaupel P and Mayer A 2007 Hypoxia in cancer: significance and impact on clinical outcome *Cancer Metastasis Rev.* **26** 225–39
[4] Nordsmark M *et al* 2005 Prognostic value of tumor oxygenation in 397 head and neck tumors after primary radiation therapy. An international multi-center study *Radiother. Oncol.* **77** 18–24
[5] Wardman P 2009 The importance of radiation chemistry to radiation and free radical biology (the 2008 Silvanus Thompson memorial lecture) *Br. J. Radiol.* **82** 89–104
[6] Zeman E M 2016 *The Biological Basis of Radiation Oncology, in Clinical Radiation Oncology* ed L L Gunderson and J E Tepper 4th edn (Philadelphia: Elsevier) ch 1, pp 2–40
[7] Bennett M H *et al* 2012 Hyperbaric oxygenation for tumour sensitisation to radiotherapy *Cochrane Database Systematic Review* **18** 05007

[8] Hoskin P, Rojas A and Saunders M 2009 Accelerated radiotherapy, carbogen, and nicotinamide (Arcon) in the treatment of advanced bladder cancer: mature results of a phase ii nonrandomized study *Int. J. Radiat. Oncol. Biol. Phys.* **73** 1425–31

[9] Janssens G O *et al* 2012 Accelerated radiotherapy with carbogen and nicotinamide for laryngeal cancer: results of a phase III randomized trial *J. Clin. Oncol.* **30** 1777–83

[10] Kaanders J H, Bussink J and van der Kogel A J 2002 ARCON: a novel biology-based approach in radiotherapy *Lancet Oncol.* **3** 728–37

[11] Mistry I N *et al* 2017 Clinical advances of hypoxia-activated prodrugs in combination with radiation therapy *Int. J. Radiat. Oncol. Biol. Phys.* **98** 1183–96

[12] Adams G E *et al* 2012 Electron-affinic sensitization VII. A correlation between structures, one-electron reduction potentials, and efficiencies of nitroimidazoles as hypoxic cell radiosensitizers. 1976 *Radiat. Res.* **178** AV183–9

[13] Masunaga S *et al* 2006 Evaluation of hypoxic cell radio-sensitizers in terms of radio-sensitizing and repair-inhibiting potential. Dependency on p53 status of tumor cells and the effects on intratumor quiescent cells *Anticancer Res.* **26** 1261–70

[14] Wardman P 2007 Chemical radiosensitizers for use in radiotherapy *Clin. Oncol.* **19** 397–417

[15] Karasawa K *et al* 2008 Efficacy of novel hypoxic cell sensitiser doranidazole in the treatment of locally advanced pancreatic cancer: long-term results of a placebo-controlled randomised study *Radiother. Oncol.* **87** 326–30

[16] Overgaard J *et al* 1989 Misonidazole combined with split-course radiotherapy in the treatment of invasive carcinoma of larynx and pharynx: report from the DAHANCA 2 study *Int. J. Radiat. Oncol. Biol. Phys.* **16** 1065–8

[17] Overgaard J *et al* 1998 A randomized double-blind phase III study of nimorazole as a hypoxic radiosensitizer of primary radiotherapy in supraglottic larynx and pharynx carcinoma. Results of the danish head and neck cancer study (DAHANCA) protocol 5–85 *Radiother. Oncol.* **46** 135–46

[18] Kapoor V K *et al* 2003 Medicinal significance of nitroimidazoles—some recent advances *J. Sci. Ind. Res.* **62** 659–65

[19] Sharma R 2011 Nitroimidazole radiopharmaceuticals in hypoxia: II. Cytotoxicity and radiosensitization applications *Curr. Radiopharm.* 379–93

[20] Overgaard J 1994 Clinical-evaluation of nitroimidazoles as modifiers of hypoxia in solid tumors *Oncol. Res.* **6** 509–18

[21] Coleman C N 1985 Hypoxic cell radiosensitizers: expectations and progress in drug development *Int. J. Radiat. Oncol. Biol. Phys.* **11** 323–9

[22] Roberts J T *et al* 1986 A clinical phase I toxicity study of Ro 03-8799: plasma, urine, tumour and normal brain pharmacokinetics *Br. J. Radiol.* **59** 107–16

[23] Saunders M E *et al* 1978 The neurotoxicity of misonidazole and its relationship to dose, half-life and concentration in the serum *Br. J. Cancer Suppl.* **3** 268–70

[24] Harrington K J *et al* 2000 Pegylated liposome-encapsulated doxorubicin and cisplatin enhance the effect of radiotherapy in a tumor xenograft model *Clin. Cancer Res.* **6** 4939–49

[25] Zhang X *et al* 2011 *In vitro* and *in vivo* study of a nanoliposomal cisplatin as a radiosensitizer *Int. J. Nanomed.* **6** 437–44

[26] Iyer A K *et al* 2006 Exploiting the enhanced permeability and retention effect for tumor targeting *Drug Discovery Today* **11** 812–8

[27] Matsumura Y and Maeda H 1986 A new concept for macromolecular therapeutics in cancer chemotherapy: mechanism of tumoritropic accumulation of proteins and the antitumor agent smancs *Cancer Res.* **46** 6387–92

[28] Nakamura Y *et al* 2016 Nanodrug delivery: is the enhanced permeability and retention effect sufficient for curing cance? *Bioconjug. Chem.* **27** 2225–38

[29] Fang J, Nakamura H and Maeda H 2011 The EPR effect: unique features of tumor blood vessels for drug delivery, factors involved, and limitations and augmentation of the effect *Adv. Drug. Deliv. Rev.* **63** 136–51

[30] Manzoor A A *et al* 2012 Overcoming limitations in nanoparticle drug delivery: triggered, intravascular release to improve drug penetration into tumors *Cancer Res.* **72** 5566–75

[31] Gasselhuber A *et al* 2012 Comparison of conventional chemotherapy, stealth liposomes and temperature-sensitive liposomes in a mathematical model *PLoS One* **7** e47453

[32] Needham D *et al* 2000 A new temperature-sensitive liposome for use with mild hyperthermia: characterization and testing in a human tumor xenograft model *Cancer Res.* **60** 1197–201

[33] Kong G *et al* 2000 Efficacy of liposomes and hyperthermia in a human tumor xenograft model: importance of triggered drug release *Cancer Res.* **60** 6950–7

[34] Yarmolenko P S *et al* 2010 Comparative effects of thermosensitive doxorubicin-containing liposomes and hyperthermia in human and murine tumours *Int. J. Hyperth.* **26** 485–98

[35] Hope M J *et al* 1985 Production of large unilamellar vesicles by a rapid extrusion procedure: characterization of size distribution, trapped volume and ability to maintain a membrane potential *Biochim. Biophys. Acta* **812** 55–65

[36] de Matos M B C *et al* 2018 Thermosensitive liposomes for triggered release of cytotoxic proteins *Eur. J. Pharm. Biopharm.* **132** 211–21

[37] Nakamura K *et al* 2012 Comparative studies of polyethylene glycol-modified liposomes prepared using different PEG-modification methods *Biochimica et Biophys. Acta (BBA)—Biomembr.* **1818** 2801–7

[38] Atyabi F *et al* 2009 Preparation of pegylated nano-liposomal formulation containing SN-38: *in vitro* characterization and *in vivo* biodistribution in mice *Acta Pharm.* **59** 133–44

[39] Akbarzadeh A *et al* 2013 Liposome: classification, preparation, and applications *Nanoscale Res. Lett.* **8** 102

[40] Chountoulesi M *et al* 2017 The significance of drug-to-lipid ratio to the development of optimized liposomal formulation *J. Liposome Res.* **20** 249–58

[41] Taggar A S *et al* 2006 Copper–topotecan complexation mediates drug accumulation into liposomes *J. Control. Release* **114** 78–88

[42] Fritze A *et al* 2006 Remote loading of doxorubicin into liposomes driven by a transmembrane phosphate gradient *Biochimica et Biophys. Acta (BBA)-Biomembr.* **1758** 1633–40

[43] Zhigaltsev I V *et al* 2005 Liposome-encapsulated vincristine, vinblastine and vinorelbine: a comparative study of drug loading and retention *J. Control. Release* **104** 103–11

[44] Tyrrell D *et al* 1976 New aspects of liposomes *Biochimica et Biophys. Acta (BBA)-Biomembr.* **457** 259–302

[45] Al-Ahmady Z S and Kostarelos K 2012 Pharmacokinetics & tissue distribution of temperature-sensitive liposomal doxorubicin in tumor-bearing mice triggered with mild hyperthermia *Biomaterials* **33** 4608–17

[46] Landon C D *et al* 2011 Nanoscale drug delivery and hyperthermia: the materials design and preclinical and clinical testing of low temperature-sensitive liposomes used in combination with mild hyperthermia in the treatment of local cancer *Open Nanomed. J.* **3** 38

[47] De Smet M *et al* 2010 Temperature-sensitive liposomes for doxorubicin delivery under MRI guidance *J. Control. Release* **143** 120–7

[48] Banno B *et al* 2010 The functional roles of poly (ethylene glycol)-lipid and lysolipid in the drug retention and release from lysolipid-containing thermosensitive liposomes *in vitro* and *in vivo J. Pharm. Sci.* **99** 2295–308
[49] Gaber M 1998 Effect of bovine serum on the phase transition temperature of cholesterol-containing liposomes *J. Microencapsulation* **15** 207–14
[50] Pradhan P *et al* 2010 Targeted temperature sensitive magnetic liposomes for thermo-chemotherapy *J. Control. Release* **142** 108–21
[51] Hosokawa T *et al* 2003 Alteration in the temperature-dependent content release property of thermosensitive liposomes in plasma *Chem. Pharm. Bull.* **51** 1227–32
[52] Joiner M C 2009 Quantifying cell kill and cell survival *Basic Clinical Radiobiology* **4** 42–55
[53] Sørensen B S *et al* 2013 Radiosensitivity and effect of hypoxia in HPV positive head and neck cancer cells *Radiother. Oncol.* **108** 500–5
[54] Adams G *et al* 1976 A correlation between structure, one electron reduction potential and efficiency of nitroimidazoles as hypoxic cell radiosensitizers *Radiat. Res.* **67** 9–20
[55] Sugie C *et al* 2005 Reevaluation of the radiosensitizing effects of sanazole and nimorazole *in vitro* and *in vivo J. Radiat. Res.* **46** 453–9
[56] Shibamoto Y *et al* 2000 Radiosensitivity of human pancreatic cancer cells *in vitro* and *in vivo*, and the effect of a new hypoxic cell sensitizer, doranidazole *Radiother. Oncol.* **56** 265–70
[57] Yasui H *et al* 2013 The prospective application of a hypoxic radiosensitizer, doranidazole to rat intracranial glioblastoma with blood brain barrier disruption *BMC Cancer* **13** 106
[58] Hall E J and Giaccia A J 2006 *Radiobiology for the Radiologist.* (Philadelphia: Lippincott Williams & Wilkins) vol 6
[59] Overgaard J, Overgaard M and Timothy A 1983 Studies of the pharmacokinetic properties of nimorazole *Br. J. Cancer* **48** 27
[60] Ranjan A *et al* 2012 Image-guided drug delivery with magnetic resonance guided high intensity focused ultrasound and temperature sensitive liposomes in a rabbit Vx2 tumor model *J. Control. Release* **158** 487–94
[61] Kato S *et al* 2012 Enhanced radiosensitization by liposome-encapsulated pimonidazole for anticancer effects on human melanoma cells *J. Nanosci. Nanotechnol.* **12** 4472–7